Urol Res (1996) 24:305–311

ORIGINAL PAPER

F. Grases · L. García-Ferragut · A. Costa-Bauzá

Study of the early stages of renal stone formation: experimental model using urothelium of pig urinary bladder

Received: 30 August 1995 / Accepted: 8 March 1996

Abstract An experimental model that enables the close simulation of conditions prevailing in the kidney during the formation of stones, using living tissue of pig urinary bladder, was developed. The results obtained clearly confirmed the importance of the antiadherent glycosaminoglycan (GAG) layer in preventing the development of solid concretions on the urothelium. Of importance was the capacity of the necrosed urothelium to act as a heterogeneous nucleant of calcium oxalate monohydrate (COM) and dihydrate (COD) crystals, demonstrating the major urolithiasic risk factor that alterations of the healthy epithelium covering the renal papilla may pose in humans. The significant increase in brushite and hydroxyapatite crystals detected on the urothelium when the pH of the artificial urine was 6.5, and the protective GAG layer was reduced or the tissue was necrosed, was also notable. The crystallization inhibitory effects caused by citrate and phytate were also studied. It was found that whereas citrate, at normal urinary concentrations, caused a slight reduction in crystallization, with phytate there was total elimination of crystallization-when it was present at very low concentrations such as 1.0 μg/ml.

Key words Calculogenesis · Calcium oxalate · Calcium phosphates · Crystallization inhibitors · Stone development

Introduction

It seems clear that at least a significant number of papillary calculi have their origin on the surface of the papillary tip as a consequence of uroepithelial alteration, or alterations, combined with other factors. The main alterations which must be considered are the reduction of the antiadherent glycosaminoglycan (GAG) layer [12], focused necrosis, i.e., because of extended analgesic consumption [1], and microinfections. Other major factors which must also be taken into account are a persistent urinary pH below 5.5 (which favors the formation of uric acid crystals) or above 6.5 (which favors the formation of calcium phosphate crystals) and a deficit of crystallization inhibitory substances [5].

Most papillary calculi acquire a typical shape, exhibiting a concave zone that corresponds to the point of attachment to the papilla [2, 4]. Calcium phosphate and organic matter are frequently found in this area. Nevertheless, these substances can hardly be considered as a stone nidus responsible for the origin of uroliths. If these substances were a stone nidus, then they would have played a relevant role in the calculus crystalline organization; this has seldom been observed. A core developed around a nidus is always situated inside the calculus and from its fine structure it may be deduced that the stone body grows on this core. Basic geometrical considerations indicate that a nidus was originally located on the papilla surface and not deep in the collecting duct or in a subepithelial position.

Consequently, it is very important to study the early stages of the development of attached crystals using models that try to reproduce the conditions found in vivo [6, 9, 10]. This is why in this study we employed an experimental device using living pig bladder tissue to study the initial stages of calcium oxalate monohydrate (COM) stone formation.

Materials and methods

Synthetic urine

The synthetic urine was prepared immediately before use by mixing equal volumes of solutions A and B in a T-type mixing chamber.

F. Grases (✉) · L. García-Ferragut · A. Costa-Bauzá
Faculty of Science, University of the Balearic Islands,
E-07071 Palma de Mallorca, Spain

Table 1 Preparation and composition of synthetic urines I and II. Synthetic urine I: pH = 5.5, I = 0.286 M, $S = (Ca)(Ox)\gamma^2/K_{sp} = 29.90$; Synthetic urine II: pH = 6.5, I = 0.278 M, $S = (Ca)(Ox)\gamma^2/K_{sp} = 13.57$. Ionic strength (I), free calcium (Ca) and oxalate (Ox) concentrations, activity coefficient of divalent ions (γ) and relative supersaturation (S) calculated with EQSTRN89

Preparation				Composition	
Solution A (g/l)		Solution B (g/l)		Ions	Concentration (M)
Synthetic urine I					
$Na_2SO_4 \cdot 10H_2O$	6.23	$NaH_2PO_4 \cdot 2H_2O$	2.41	Na^+	$1.55 \cdot 10^{-1}$
$MgSO_4 \cdot 7H_2O$	1.46	$Na_2HPO_4 \cdot 12H_2O$	5.60	Mg^{2+}	$2.96 \cdot 10^{-3}$
NH_4Cl	4.64	NaCl	13.05	NH_4^+	$4.33 \cdot 10^{-2}$
KCl	12.13	$Na_2C_2O_4$	0.1608	K^+	$8.15 \cdot 10^{-2}$
$CaCl_2 \cdot 3.5H_2O$	3.04			Ca^{2+}	$8.75 \cdot 10^{-3}$
				SO_4^{2-}	$1.26 \cdot 10^{-2}$
				Cl^-	$2.53 \cdot 10^{-1}$
				$H_2PO_4^-$	$7.70 \cdot 10^{-3}$
				HPO_4^{2-}	$7.80 \cdot 10^{-3}$
				$C_2O_4^{2-}$	$6.00 \cdot 10^{-4}$
Synthetic urine II					
$Na_2SO_4 \cdot 10H_2O$	6.23	$NaH_2PO_4 \cdot 2H_2O$	2.41	Na^+	$1.55 \cdot 10^{-1}$
$MgSO_4 \cdot 7H_2O$	1.46	$Na_2HPO_4 \cdot 12H_2O$	5.60	Mg^{2+}	$2.96 \cdot 10^{-3}$
NH_4Cl	4.64	NaCl	13.05	NH_4^+	$4.33 \cdot 10^{-2}$
KCl	12.13	$Na_2C_2O_4$	0.0804	K^+	$8.15 \cdot 10^{-2}$
$CaCl_2 \cdot 3.5H_2O$	2.40			Ca^{2+}	$6.90 \cdot 10^{-3}$
				SO_4^{2-}	$1.26 \cdot 10^{-2}$
				Cl^-	$2.43 \cdot 10^{-1}$
				$H_2PO_4^-$	$7.70 \cdot 10^{-3}$
				HPO_4^{2-}	$7.80 \cdot 10^{-3}$
				$C_2O_4^{2-}$	$3.00 \cdot 10^{-4}$

Both solutions were prepared by dissolving chemicals of reagent-grade purity in deionized and redistilled water. Once prepared, solutions were sterilized by filtering through filters with 0.2-μm pores. Solutions were stored for a maximum of 1 week at 4 °C. Two different compositions of synthetic urine were prepared. Their compositions, pH values, ionic strengths and relative supersaturations are given in Table 1.

Physiological salt solution

Earle's physiological salt solution was prepared immediately before use by mixing the appropriate volumes of concentrated stock solution stored for a maximum of 1 week at 4 °C and adjusting the pH to 7.2. Once prepared, solution was sterilized by filtering through filters with 0.2-μm pores. In all the experiments the physiological salt solution was aerated with an $O_2 + 5\%$ CO_2 gas mixture. Earle's physiological salt solution contained $1.16 \cdot 10^{-1}$ M NaCl, $5.36 \cdot 10^{-3}$ M KCl, $1.79 \cdot 10^{-3}$ M $CaCl_2 \cdot 2H_2O$, $8.11 \cdot 10^{-4}$ M $MgSO_4 \cdot 7H_2O$, $1.02 \cdot 10^{-3}$ M $NaH_2PO_4 \cdot 2H_2O$, $2.00 \cdot 10^{-2}$ M $NaHCO_3$ and $5.55 \cdot 10^{-3}$ M glucose.

Specimens

Urinary bladders from freshly slaughtered 2-month-old pigs were transferred aseptically to the laboratory in ice-cold 0.9% sodium chloride solution. This solution was supplemented with 100 μg/ml streptomycin, 100 μg/ml amoxicillin and 20 μg/ml clavulanic acid in order to eradicate proliferation of bacteria, especially the *E. coli* strains that colonize the alimentary tract of most warm-blooded animals. After being placed on ice and under sterile conditions, urinary bladder was excised mechanically and opened by a longitudinal incision. The cut tissue was rinsed twice with 0.9% saline solution to remove residual urine. It was then placed on a 6.5-cm-diameter rubber ring, with the outer part of the bladder in contact with the ring, and fixed with needles. Experiments were performed with control bladders (bladders without injury) and injured bladders. Chemical and physical injuries of the inner part of the bladder were induced by 0.1 N HCl at 25 °C for 2 min and gentle drying in a desiccator at 25 °C for 24 h, respectively.

Simulation of the early stages of crystal formation

Experiments were carried out in a methacrylate cylindrical flask 6 cm in inner diameter and 10 cm high with a tissue holder situated 5 cm from the bottom, and equipped with appropriate holes for the input and evacuation of synthetic urine and physiological salt solution. The tissue bladder, fixed at the rubber ring, was situated in the flask with its inner part facing the top and the flask was placed in a temperature-controlled chamber at 37 °C. Freshly prepared synthetic urine was introduced at a rate of 780 ml/day, by a multichannel peristaltic pump, into the upper part of the flask. Using the same multichannel peristaltic pump, aerated physiological salt solution was introduced, at a rate of 390 ml/day, into the lower part of the flask. Both solutions were kept at 37 °C in a thermostatic bath (Fig. 1). The system was operated for 8 h. When the experiment was finished the piece of tissue was removed from the system, quickly rinsed in 0.9% saline solution to remove any crystals which were not firmly adhered and divided into two square pieces. One piece of tissue was fixed with needles to a piece of wax and underwent microscopic study. The other piece underwent a viability test in order to predict survival.

Effect of various compounds

The effects of citrate (supplied by Probus) at 600 μg/ml and phytate (supplied by Sigma) in the concentration range 0.05–1.00 μg/ml were

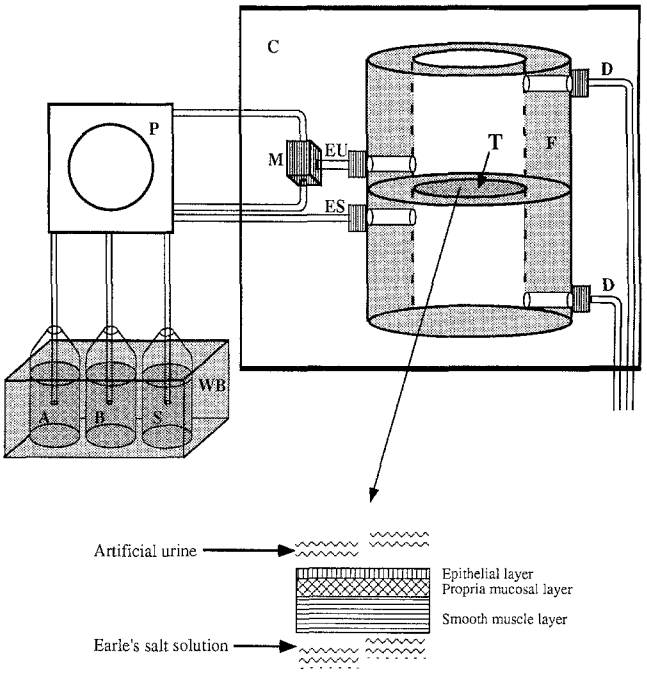

Fig. 1 Schematic diagram of the model used to simulate renal stone formation on pig bladder tissue. *A* Solution A for artificial urine preparation, *B* solution B for artificial urine preparation, *S* aerated Earle's physiological salt solution, *WB* constant temperature water bath. *P* peristaltic pump, *C* temperature-controlled chamber, *F* methacrylate cylindrical flask, *M* T-type mixing chamber, *EU* entrance for synthetic urine, *ES* entrance for physiological salt solution, *D* drainpipes, *T* piece of tissue

assayed by the addition of different amounts of these substances to the synthetic urine. Phytic acid is a natural product found in some vegetable seeds and mammalian tissues, with noteworthy effects on the inhibition of calcium oxalate crystallization which were recently described [4, 7] and, for this reason, phytic acid was included in the present study. Considering the normal range of urinary pH values, phytic acid is mainly found in the urine as the dissociated form, i.e., as phytate. As explained previously [7], due to the high concentrations of citrate used and considering its capacity to complex calcium ions, in experiments in which the action of citrate ions was evaluated, a calcium supplement was added to obtain the same calcium oxalate supersaturation value as that found in the absence of citrate.

Screening for contamination

After each experiment, all solutions were cultured with conventional microbiological culture techniques on tryptic soy agar. This isolation medium has been suggested by the United States Pharmacopeia (1985) and by the European Pharmacopeia (1980) as being suitable for demonstrating the presence of viable forms of bacteria, fungi and yeast. Parallel positive (broth culture of *Bacillus subtilis*) and negative controls (sterile water) were cultured on the same medium. Samples were incubated at 37 °C and observed every working day over 3 days for signs of growth.

Viability test

Cuts were made in the sheet of tissue to produce a strip to which a thread was attached at each end and the preparation mounted in a 50-ml organ bath with Earle's physiological salt solution at 37 °C. One end was tied to a fixed pin that was hollow and served as an aerator. The other end of the preparation was attached to a lever force-displacement transducer fitted with a writing point which marked the paper attached to the drum of a kymograph. When a steady baseline was obtained, 2 ml 10^{-6} M acetylcholine was added. A sustained contraction of the tissue demonstrated the ability of the bladder cells to survive.

A dye exclusion assay with trypan blue, a viability dye which has been used to determine membrane integrity, was also applied to measure tissue survival. This method is based on the principle that live (viable) cells do not take up the dye, whereas dead (nonviable) cells do. A cell suspension in Earle's physiological salt solution was prepared with a sheet of tissue, and 0.5 ml 0.4% trypan blue solution, 0.5 ml Earle's physiological salt solution and 0.2 ml cell suspension were transferred to a test tube. The mixture was thoroughly mixed and allowed to stand for 5 min. Percentage cell viability (total viable cells/total cells × 100) was determined by counting the cells with a standard hemocytometer chamber. In all experiments percentage cell viability was over 60%.

Microscopic observation of attached crystals

For scanning electron microscopy, specimens were immersion fixed in 2.5% glutaraldehyde with 0.1 M cacodylate sodium buffer (pH = 7.3) at 4 °C, postfixed with 2% osmium tetraoxide in the same buffer, dehydrated in a graded acetone series and then dried in an autocritical point drier. After coating with gold, the surface of the samples was examined with a scanning electron microscope (Hitachi S-530) equipped with energy-dispersive X-ray microanalysis.

Quantification of attached crystals

Once samples had undergone microscopic study, tissues were cut into 2.25-cm^2 pieces and placed in a glass tube with 0.6 ml HNO_3 : HCl (1 : 3) at room temperature for 30 min. Solutions were then completed with 4 ml redistilled water and analyzed for calcium and phosphorus content using an atomic emission spectrometer with inductively coupled plasma (Perkin-Elmer 2000). The amount of calcium and phosphorus per unit weight of tissue in normal pig bladder was evaluated following the previous procedure in non-incubated samples with the same area and different weights. By subtracting these values from the amount of calcium and phosphorus in the incubated bladders it was possible to calculate the amount of calcium and phosphorus that had adhered to the bladder wall.

Results

The designed experimental model enabled a living tissue of pig urinary bladder to be maintained, for 8 h at least, in contact with flowing artificial urine. It is interesting to observe that during this time no crystals of any type were formed on the tissue surface when normocalciuric artificial urine at pH 5.5 was used, and only very few crystals of calcium oxalate dihydrate were detected using hypercalciuric artificial urine at pH 5.5 (Fig. 2). Nevertheless, when the protective GAG layer that covers the inner urothelium of the pig bladder had been previously removed by washing with 0.1 N HCl, using an artificial hypercalciuric urine at pH 5.5, a significant amount of primary aggregates of

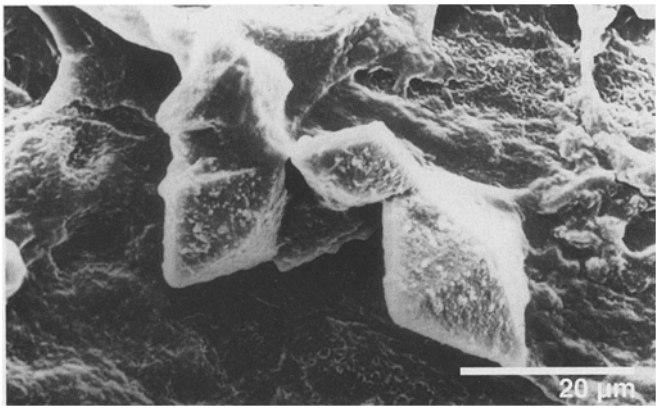

Fig. 2 Calcium oxalate dihydrate crystals observed on the surface of healthy tissue when using hypercalciuric artificial urine at pH 5.5 (SEM image)

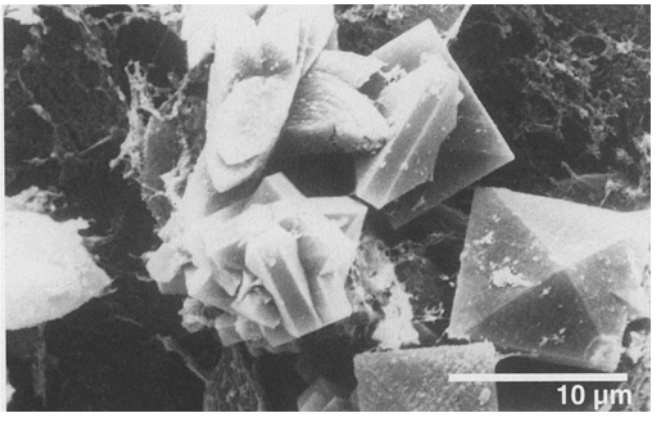

Fig. 3 Primary aggregates of calcium oxalate monohydrate and dihydrate observed on the surface of a tissue with injuries induced by 0.1 N HCl when using hypercalciuric artificial urine at pH 5.5 (SEM image)

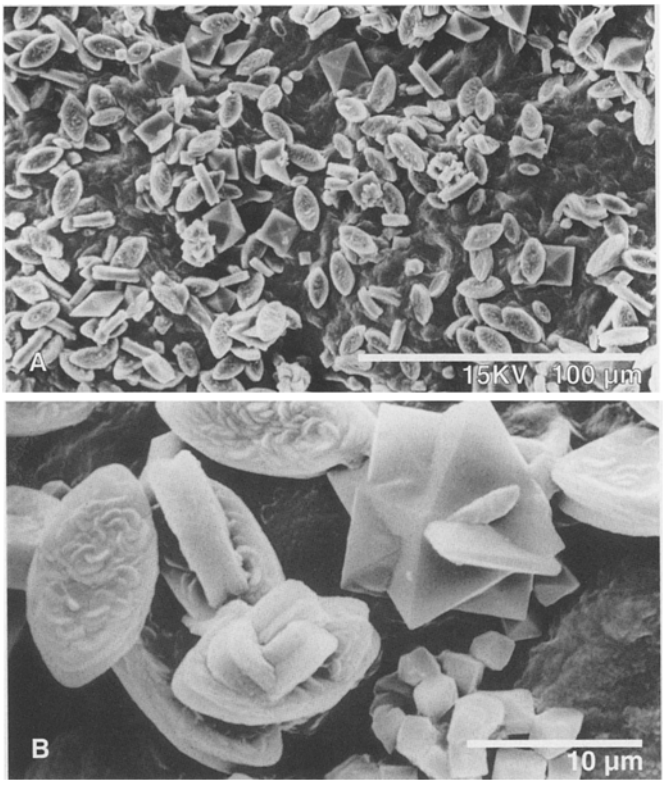

Fig. 4A, B Primary aggregates of calcium oxalate monohydrate and dihydrate observed on the surface of a tissue with injuries induced by drying in a desiccator when using hypercalciuric artificial urine at pH 5.5. **A** General view, **B** detail (SEM images)

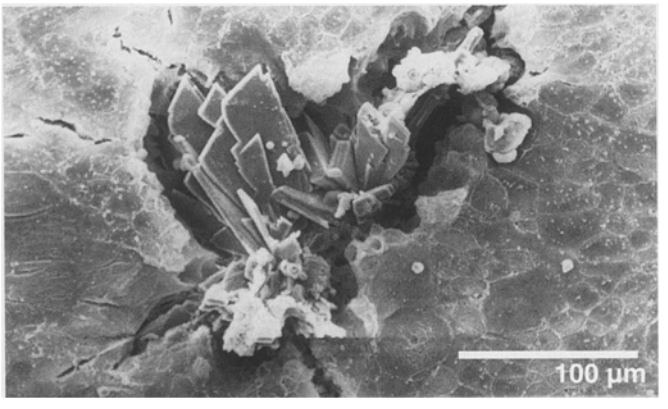

Fig. 5 Isolated aggregates of brushite crystals observed on the surface of healthy tissue when using normocalciuric artificial urine with a pH of 6.5 (SEM image)

COM and COD crystals were observed on the apical side (Fig. 3). Using totally necrosed urothelial tissue and an artificial hypercalciuric urine at a pH of 5.5, all the necrosed surface appeared fully covered with COM and COD crystals (Fig. 4). These experiments clearly demonstrated that crystals that appeared on the urothelial tissue, when it was damaged, were directly formed on this tissue as a consequence of interactions between normally supersaturated urine and tissue, and did not appear as a result of interactions between preformed crystals and tissue, due to the deposition of previously formed crystals.

Experiments performed using noninjured pig bladder urothelium and normocalciuric artificial urine with a pH of 6.5 showed the formation of some isolated aggregates of brushite crystals (Fig. 5). When the same experiment was performed using a pig bladder urothelium with previous elimination of the protective GAG layer, a significant quantity of brushite and hydroxyapatite was detected (Fig. 6). It is interesting to observe the presence of COD crystals nucleated on the brushite. Using totally necrosed urothelial tissue and a normocalciuric artificial urine at a pH of 6.5, all the surface appeared covered with brushite and hydroxyapatite (Fig. 7).

The effects of citrate and phytate on the crystal development on pig bladder urothelium using

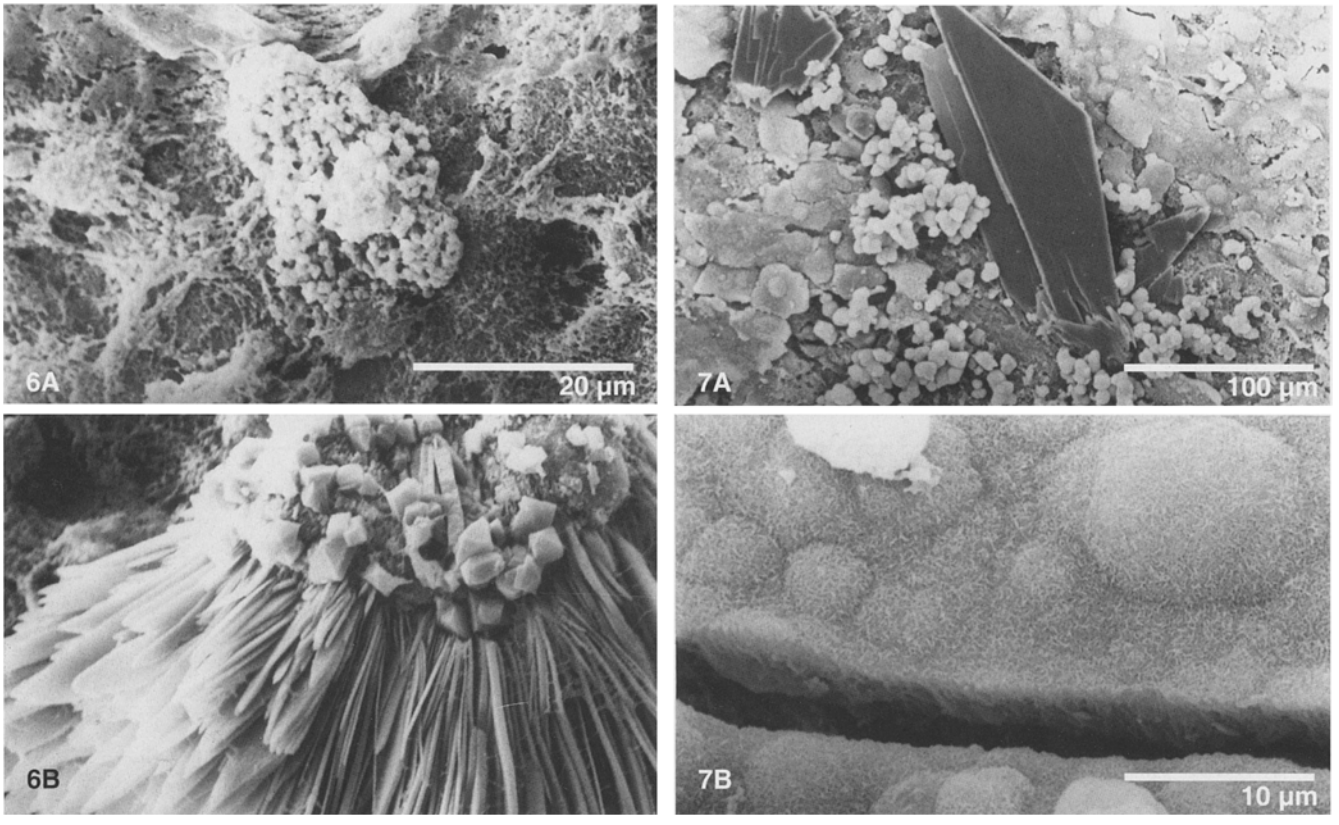

Fig. 6A, B Brushite and hydroxyapatite crystals observed on the surface of a tissue with injuries induced by 0.1 N HCl when using normocalciuric artificial urine with a pH of 6.5. **A** Aggregates of spherulitic hydroxyapatite (SEM image). **B** Calcium oxalate dihydrate crystals nucleated on the brushite (SEM image)

Fig. 7 **A** Brushite and hydroxyapatite crystals observed on the surface of tissue with injuries induced by drying in a desiccator when using normocalciuric artificial urine with a pH of 6.5 (SEM image). **B** Detail of the surface, which is totally covered with hydroxyapatite (SEM image)

hypercalciuric artificial urine at pH 5.5 are shown in Fig. 8. As can be seen, whereas the presence of citrate at normal urinary concentrations, 600 µg/ml, caused only a slight decrease in the amount of developed crystals in the three situations studied (healthy urothelium, urothelium without the protective GAG layer and necrosed urothelium), the phytate provoked a dramatic decrease in the tissue calcification in such a manner that a concentration as low as 0.5 µg/ml totally eliminated crystal development. It is interesting to point out that minimum phytate effects were detected for concentrations around 0.1 µg/ml and these effects were more noticeable on necrosed urothelium.

The effects of phytate on crystal formation on pig bladder urothelium using normocalciuric artificial urine at pH 6.5 are shown in Fig. 9. As can be seen, the presence of small amounts of phytate caused significant inhibitory effects on the development of calcium phosphate crystals (brushite and hydroxyapatite) such that a concentration as low as 1 µg/ml phytate totally eliminated the development of these crystals. Similarly to the above-described experiments, the inhibitory effects were more noticeable on necrosed urothelium and no effects were detected when phytate concentrations were less than 0.1 µg/ml.

Discussion

The system described in this paper enables the simulation of conditions prevailing in the kidney during the formation of stones using living renal epithelial tissue. The main advantages of this device are that it allows the study of the interactions between the epithelial cells and crystals as a function of the state of the renal tissue and as a function of the urine composition. It should be considered that the living tissue mainly acts as a heterogeneous nucleant and this capacity depends on its specific characteristics such as its antiadherent capacity, its crystal endocytosis capacity and its retention of supersaturated liquids. Thus, the results presented confirm the importance of the antiadherent GAG layer in preventing the development of solid concretions on the urothelium. Thus it is very interesting to compare the results obtained using living urothelium with those

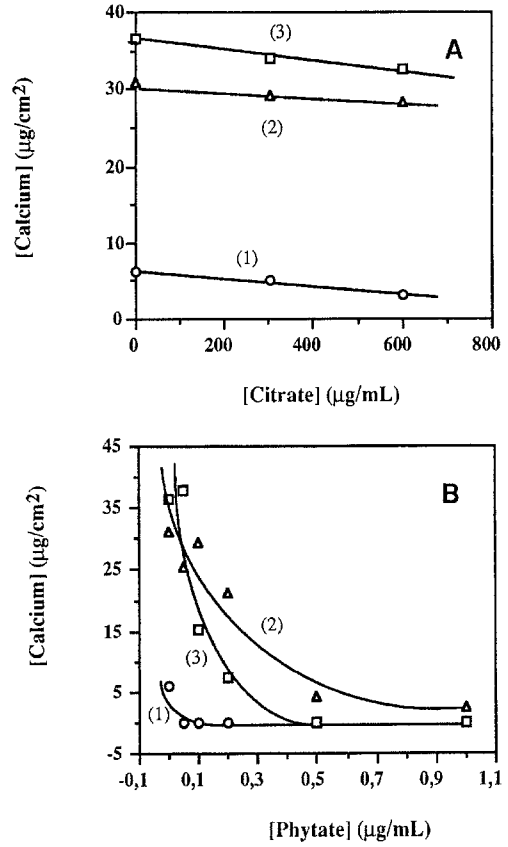

Fig. 8A, B Effects of citrate and phytate on crystal development on *1* healthy bladder urothelium, *2* bladder urothelium with the GAG layer partially removed and *3* necrosed bladder urothelium, when using hypercalciuric artificial urine with a pH of 5.5. **A** Amount of calcium adhered to the bladder wall vs. citrate concentration. **B** Amount of calcium adhered to the bladder wall vs phytate concentration

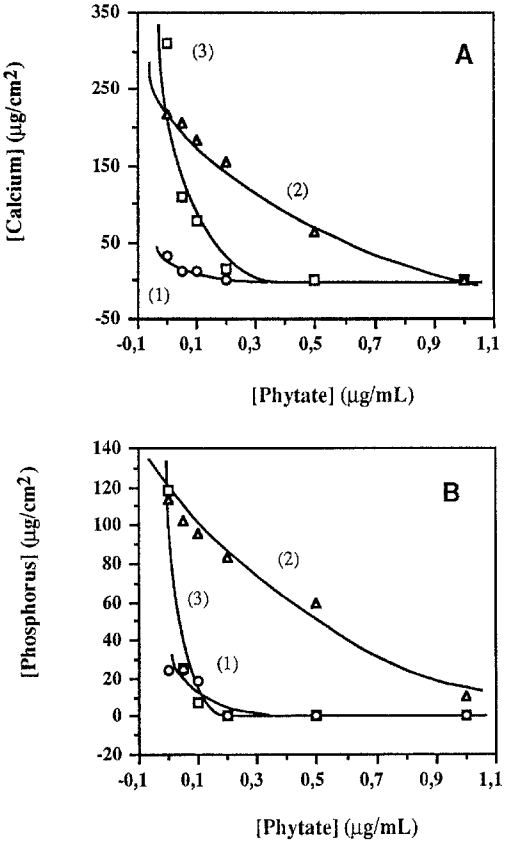

Fig. 9A, B Effect of phytate on crystal development on *1* healthy bladder urothelium, *2* bladder urothelium with the GAG layer partially removed and *3* necrosed bladder urothelium, when using normocalciuric artificial urine with a pH of 6.5. **A** Amount of calcium adhered to the bladder wall vs phytate concentration. **B** Amount of phosphorus adhered to the bladder wall vs phytate concentration

found using the same tissue but with removal of the protective GAG layer, by washing with diluted HCl [3, 8], or with the results obtained using necrosed tissue (by drying). As commented in "Results", in a healthy urothelium no crystals were detected using normocalciuric artificial urine at pH 5.5 and only a few crystals were found in hypercalciuric/hyperoxaluric conditions at the same pH (Fig. 2). Nevertheless, when the protective GAG layer was reduced, by washing with 0.1 N HCl, a significant increase in the number of primary aggregates of COM and COD crystals formed on the tissue was observed (Fig. 3). This solid concretion development was still more noticeable on necrosed tissue where the protective and antiadherent GAG layer was totally nonexistent (Fig. 4). This fact also demonstrated the significant capacity of the necrosed urothelium to act as heterogeneous nucleant of COM and COD crystals and consequently the significant urolithogenic risk factor that the necrosis of renal tissue poses.

Likewise, the significant increase in brushite and hydroxyapatite crystals is remarkable that was detected on the urothelium when the pH of normocalciuric artificial urine was 6.5 and the protective GAG layer was reduced by HCl washing (Fig. 6). This increase was still more remarkable on necrosed urothelial tissue (Fig. 7). These facts demonstrate the important lithiasic risk factor that must be involved with persistent urinary pH values of up to 6.5.

The crystallization inhibitory effects caused by citrate and phytate using an artificial hypercalciuric/hyperoxaluric urine at pH 5.5 (Fig. 8) demonstrated that, whereas citrate only caused a slight reduction of the formed calcium crystals, phytate totally eliminated calcium crystals when it was present at very low concentrations such as 0.5 µg/ml. Phytate is a hexaphosphate of inositol that occurs naturally in some plant seeds; thus most wheat bran contains between 4% and 5% phytate. Other phytate plant sources are wild rice, corn, soybeans, sesame seeds, and pistachios. Inositol phosphates are also contained in mammalian cells, acting as intracellular messengers that link receptor activation to Ca^{2+} mobilization [11]. Between 1% and 10% of the total ingested phytate is excreted by the urine. In this regard it is important to consider that due to the

modern tendency to consume refined meals (bread, rice, etc.) the actual ingestion of phytate has been notably reduced. This then is an aspect that must be considered in further studies.

As is shown in Fig. 9, phytate also caused a significant inhibition of calcium phosphate crystallization on pig bladder epithelial tissue. Thus, whereas in the absence of phytate considerable amounts of brushite and hydroxyapatite were detected on the epithelium with the reduced GAG layer and on the necrosed epithelium, the presence of 1.0 μg/ml phytate totally prevented the deposit of calcium phosphate. This inhibitory action must be related to the affinity of phosphate groups with the calcium and to the particular chemical ring structure of the phytate that, through adsorption processes, causes significant disturbances of calcium oxalate crystal nucleation and growth. Moreover, it is interesting to observe that the phytate inhibitory action was more noticeable on the necrosed epithelium than in the epithelium with the reduced GAG layer.

Acknowledgements The financial support of the Dirección General de Investigación Científica y Técnica (grant PB 92-0249) is gratefully acknowledged. Veterinary service of the local slaughterhouse Escorxadors i Industries Carniques de la Conselleria de Sanitat del Govern Balear is also gratefully acknowledged for the biological material supplying.

References

1. Brenner BM, Rector FC (1976) The kidney. WB Saunders, Philadelphia, II:1640
2. Cifuentes L, Miñón J, Medina JA (1987) New studies on papillary calculi. J Urol 137:1024
3. Gill WB, Ruggiero K, Straus FH (1979) Crystallization studies in a urothelial-lined living test tube (the catheterized female rat bladder). I. Calcium oxalate crystal adhesion to the chemically injured rat bladder. Inv Urol 17:257
4. Grases F, Costa-Bauzá A, Conte A (1993) Studies on structure of calcium oxalate monohydrate renal papillary calculi. Mechanism of formation. Scanning Microsc 7:1067
5. Grases F, Costa-Bauzá A, March JG, Söhnel O (1993) Artificial simulation of renal stone formation. Influence of some urinary components. Nephron 65:77
6. Grases F, Costa-Bauzá A, March JG (1994) Artificial simulation of the early stages of renal stone formation. Br J Urol 74:298
7. Grases F, García-Ferragut L, Costa-Bauzá A, March JG (1996) Study of the effects of different substances on the early stages of papillary stone formation. Nephron (in press)
8. Grenabo L, Hedelin H, Hugosson J, Pettersson S (1988) Adherence of urease-induced crystals to rat bladder epithelium following acute infection with different uropathogenic microorganisms. J Urol 140:428
9. Lieske JC, Toback FG (1993) Regulation of renal epithelial cell endocytosis of calcium oxalate monohydrate crystals. Am J Physiol 264:F800
10. Mandel N, Riese R (1991) Crystal-cell interactions: crystal binding to rat renal papillary tip collecting duct cells in culture. Am J Kidney Dis XVII:402
11. Menniti FS, Oliver KG, Putney JW Jr, Shear SB (1993) Inositol phosphates and cell signaling: new views of $InsP_5$ and $InsP_6$. Trends Biochem Sci 18:53
12. See WA, Williams RD (1992) Urothelial injury and clotting cascade activation: common denominators in particulate adherence to urothelial surfaces. J Urol 147:541